EXTENDED PDF FORMAT
SPONSORED BY

BIO-RAD

http://discover.bio-rad.com



Small Mid-Pleistocene Hominin Associated with East African Acheulean Technology

Richard Potts, *et al.*

Science **305**, 75 (2004);
DOI: 10.1126/science.1097661

The following resources related to this article are available online at www.sciencemag.org (this information is current as of January 2, 2007):

Updated information and services, including high-resolution figures, can be found in the online version of this article at:
http://www.sciencemag.org/cgi/content/full/305/5680/75

Supporting Online Material can be found at:
http://www.sciencemag.org/cgi/content/full/305/5680/75/DC1

A list of selected additional articles on the Science Web sites **related to this article** can be found at:
http://www.sciencemag.org/cgi/content/full/305/5680/75#related-content

This article **cites 12 articles**, 3 of which can be accessed for free:
http://www.sciencemag.org/cgi/content/full/305/5680/75#otherarticles

This article has been **cited by** 6 article(s) on the ISI Web of Science.

This article appears in the following **subject collections**:
Anthropology
http://www.sciencemag.org/cgi/collection/anthro

Information about obtaining **reprints** of this article or about obtaining **permission to reproduce this article** in whole or in part can be found at:
http://www.sciencemag.org/help/about/permissions.dtl

Downloaded from www.sciencemag.org on January 2, 2007

Science (print ISSN 0036-8075; online ISSN 1095-9203) is published weekly, except the last week in December, by the American Association for the Advancement of Science, 1200 New York Avenue NW, Washington, DC 20005. Copyright c 2006 by the American Association for the Advancement of Science; all rights reserved. The title SCIENCE is a registered trademark of AAAS.

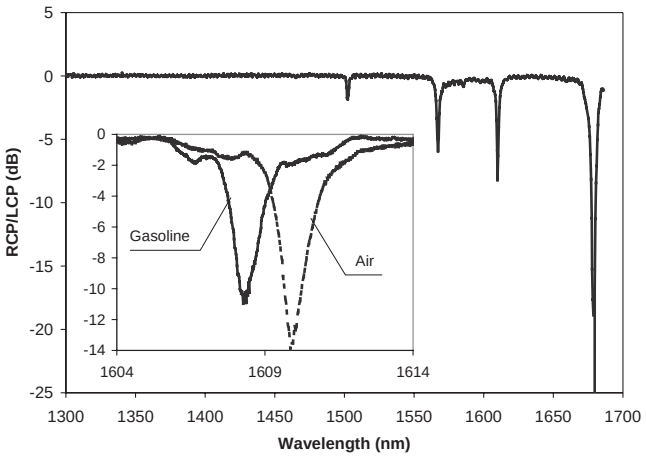


Fig. 3. Ratio of RCP to LCP transmission through a CLPG. To perform the optical measurements, we placed the fibers inside hollow metallic tubes with a standard fiber-optic ferrule at each end. The ends of the fiber were glued with epoxy into the ferrules and polished. An Agilent 83437A broadband light source was used for spectral measurements in the 1250- to 1700-nm spectral range. The light from the source was collimated by a gradient index. (GRIN) lens and focused into the sample fiber core with a 100× microscope objective. The polarization state of light was controlled by a thin-film polarizer and a zero-order quarter-wave plate. The output light was collected by a 100× objective and then directed to a receiving GRIN lens pigtailed with a fiber connected to an Agilent optical spectrum analyzer 86145B. The inset illustrates the shift of a transmission dip when the CLPG is surrounded by gasoline.

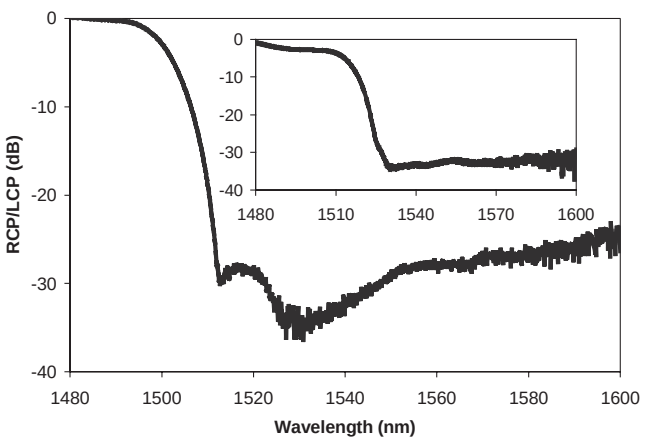


Fig. 4. Ratio of RCP to LCP transmission through a CIPG. The inset shows the ratio for a broadband in-fiber polarizer based on a CIPG with nonuniform pitch.

These were a 55-mm-long CLPG with a pitch of 78 μm (sample 1) and an 11-mm-long CIPG with a pitch of 45 μm (sample 2). The ratio of right circularly polarized (RCP) to left circularly polarized (LCP) transmission through sample 1 (Fig. 3) shows that although LCP light is not affected by the right-handed structure, RCP light displays dips in transmission similar to those observed in standard LPG structures. The spectral positions of these dips coincide with the wavelength of scattering of the core mode into copropagating cladding modes for the second diffraction order of the conventional LPG. The transmission dip shifts when the CLPG is surrounded by gasoline (Fig. 3, inset).

The ratio of RCP to LCP transmission through sample 2, which acts as a CIPG, is shown in Fig. 4. The amplitude of oscillation in the band may be smoothed by varying the pitch (Fig. 4, inset). The long wavelength edge of the scattering band in a chiral rod has been observed previously in microwave measurements (*3*). The present optical measurements cover the short wavelength edge of a scattering band. This suggests the CIPG may serve as a broadband polarizer.

References and Notes

1. A. Othonos, K. Kalli, *Fiber Bragg Gratings: Fundamentals and Applications in Telecommunications and Sensing* (Artech, Norwood, MA, 1999).
2. K. P. Chen, P. R. Herman, R. Tam, *IEEE Photon. Technol. Lett.* **14**, 170 (2002).
3. V. I. Kopp, A. Z. Genack, *Opt. Lett.* **28**, 1876 (2003).
4. S. C. Rashleigh, *IEEE J. Lightwave Technol.* **LT-1**, 312 (1983).
5. D. A. Nolan, M. N. Islam, U.S. Patent 6,229,937 (2001).
6. R. Ulrich, A. Simon, *Appl. Opt.* **18**, 2241 (1979).
7. H. Huang, *Appl. Opt.* **36**, 6968 (1997).
8. V. Bhatia, A. M. Vengsarkar, *Opt. Lett.* **21**, 692 (1996).
9. V. Grubsky, A. Skorucak, D. S. Starodubov, J. Feinberg, *IEEE Photonics Technol. Lett.* **11**, 87 (1999).
10. We thank C. Draper for help in preparing CLPGs. Supported by the U.S. Department of Commerce, National Institute of Standards and Technology, Advanced Technology Program, cooperative agreement no. 70NANB3H3038 and by the National Science Foundation under grant no. DMI-0340149.

8 March 2004; accepted 12 May 2004

Small Mid-Pleistocene Hominin Associated with East African Acheulean Technology

Richard Potts,[1,2]* Anna K. Behrensmeyer,[3] Alan Deino,[4] Peter Ditchfield,[5] Jennifer Clark[1]

Hominin fossils from the African mid-Pleistocene are rare despite abundant Acheulean tools in Africa and apparently African-derived hominins in Eurasia between 1.0 and 0.5 million years ago (Ma). Here we describe an African fossil cranium constrained by $^{40}Ar/^{39}Ar$ analyses, magnetostratigraphy, and sedimentary features to 0.97 to 0.90 Ma, and stratigraphically associated with Acheulean handaxes. Although the cranium represents possibly the smallest adult or near-adult known between 1.7 and 0.5 Ma, it retains features observed in larger *Homo erectus* individuals, yet shows a distinct suite of traits indicative of wide population variation in the hominins of this period.

African hominin fossils dating to between 1.0 and 0.5 million years ago (Ma) are sparse despite widespread Acheulean artifacts in this period. The African sample between roughly 1.5 and 1.0 Ma includes partial crania from Olduvai (OH 9), Tanzania; Daka, Ethiopia; and Buia, Eritrea (*1–5*). Later specimens of African *Homo* include the ~0.6-million-year-old cranium from Bodo, Ethiopia, and uncalibrated specimens from Kabwe, Zambia; Ndutu, Tanzania; and Saldanha, South Africa (*6–9*). The relationship of African *Homo* to East Asian *Homo erectus*, dated between 1.7 and 0.5 Ma, and to European fossils, dated perhaps 0.9 to 0.8 Ma, is contested (*1*, *10–13*). The entire sample of fossils from Africa, Asia, and Europe exhibits wide morphological variation that some researchers divide into multiple lineages and others place in a single polytypic species (*14–16*). Here we describe a cranium dating to 0.97 to 0.90 Ma from Olorgesailie, Kenya, that helps compare these older and younger hominin fossils.

The partial cranium designated KNM-OL 45500 was found in the same stratigraphic level as the rich Acheulean handaxe sites of Olorgesailie, Kenya (*17*). The specimen consists of the frontal and left temporal bones and nine cranial vault fragments (Fig. 1). The frontal bone was found in situ in June 2003 in

Downloaded from www.sciencemag.org on January 2, 2007

a sediment block that was excavated and removed from the site in August 1999. Other parts of the cranium were discovered 1 to 20 m downslope of the in situ frontal from 28 July through 22 August 2003 by M. Kanunga, C. M. Kilonzi, R. Kinyua, J. Kioko, G. Mumo, J. M. Nume, and R. Potts. Although Olorgesailie preserves dense accumulations of Acheulean stone artifacts and mammalian fossils, KNM-OL 45500 is the first hominin discovered at the site since initial exploration in 1942 (*17*, *18*).

The block containing the frontal was derived from sediments that onlap the east side of a prominent volcanic ridge (Lava Hump) connecting the Mt. Olorgesailie foothills to the lowland basin (Fig. 2). The fossil was covered in poorly sorted sandy silt that contained angular volcanic sand, and its lower surface rested on well-sorted silt of an underlying paleosol. These sediments represent the boundary between Members 6/7 and Member 5 of the Olorgesailie Formation, which can be traced laterally to excavations along Lava Hump and elsewhere in the basin.

The age of the fossil layer is constrained by radiometric ages for overlying and underlying volcanic units and by magnetostratigraphy. Single-crystal $^{40}Ar/^{39}Ar$ dating of large pumice clasts from the lower part of Member 5 yielded an age of 974 ± 7 thousand years ago (ka), whereas a crack-filling air-fall ash at the top of Member 8 yielded 747 ± 6 ka (*19*) (Fig. 2). The Matuyama-Brunhes magnetostratigraphic transition is recorded in fine-grained sediments near the base of Member 8 (*20*). The age of this transition is approximately 790 ka (*21*, *22*). An interval of ~182,000 years is thus represented between the base of Member 8 and the lower Member 5 pumice. Much of this sequence probably formed after the hominin fossil, which is overlain by a well-developed laterally extensive paleosol at the top of Member 7 and an erosive contact between Members 8 and 7 (*18*). Because there is no sedimentary evidence for a major hiatus between the lower date and the hominin level, we estimate the age of the Member 5/7 boundary and the hominin fossil as closer to the lower age of 974 ka; that is, between 970 and 900 ka (Fig. 2).

The nearly complete frontal bone includes the supraorbital torus, most of the squama with a well-preserved frontal crest, the anterior portions of the orbital roofs, and the interorbital area with a large rectangular frontal sinus exposed inferiorly. The temporal bone preserves the entire squamous and mastoid portions. The zygomatic process is broken near its root, leaving an 8-mm-wide shelf of the zygomatic root medial to the fracture. The mandibular fossa is intact and exhibits a small but distinct postglenoid process and a small articular tubercle (Fig. 1).

KNM-OL 45500 was a small individual but with sufficient development of bony superstructures to warrant designation as an adult or near-adult. The post-toral sulcus is as developed relative to the rest of the frontal bone as in adult *H. erectus*. The convex interorbital region is as wide as in adults of early African *H. erectus* and is more prominent (as measured by glabella height) than in adults, including massive crania, of mid-Pleistocene *Homo*. Although the cranial vault is thin overall, the mid-squama thickness of the frontal vault is typical for adults such as KNM-ER 3733 from Turkana and OH 9 from Olduvai. The mastoid process of the temporal bone is crested, and its tip projects below the occipitomastoid suture. The root of the zygomatic arch is as strongly developed as in KNM-ER 3733 and Kabwe and is larger than in the juvenile KNM-WT 15000. Although the cranial sutures of KNM-OL 45500 tend to be broken or eroded, the sphenotemporal suture is closed but the left lateral portion of the coronal suture is not (Fig. 1).

Despite this evidence of adult or near-adult status, KNM-OL 45500 exhibits the smallest frontal breadth, supraorbital torus thickness and breadth, and overall temporal bone size of any early- or middle-Pleistocene adult cranium (table S1). Lateral to the prominent glabellar region and large frontal sinus, the supraorbital torus is thinner vertically than in adult *H. erectus*. The mandibular fossa exhibits mature development (*23*), yet is the smallest in mid-Pleistocene adult hominins despite its position beneath the relatively large zygomatic root. Although the mastoid process bears two distinct vertically oriented crests, it is slender and is not associated with a supramastoid crest, which typifies larger adults of mid-Pleistocene *Homo*.

Two specimens from Dmanisi (the near-adult D2282 and adult D2280) closely match the frontal torus/vault and temporal bone size of KNM-OL 45500 (*24*), and the supraorbital torus of OH 12 from Olduvai approximates the size of the Olorgesailie fossil (*25*). The former two crania, about 1.75 million years old, have among the smallest cranial capacities of *H. erectus*–like individuals, approximated at 650 and 780 cc (*24*), implying that

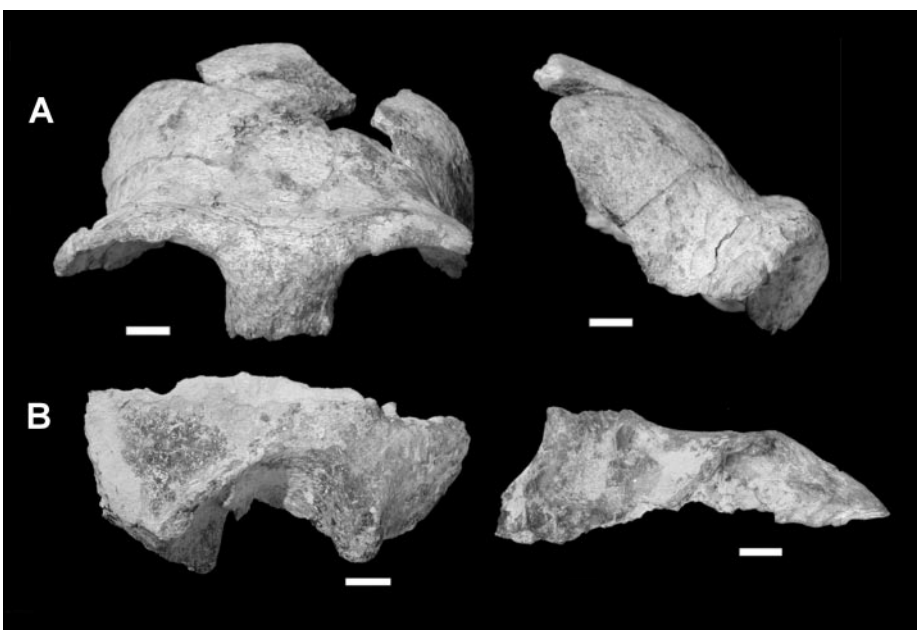


Fig. 1. Partial hominin cranium, KNM-OL 45500, from Olorgesailie. Scale bars equal 1 cm. (**A**) Frontal bone, anterior view (left) and right lateral view (right). The squama is broken roughly 10 mm anterior to the bregma and along most of the coronal suture. The lateral portion of the left supraorbital region, near the anterior root of the temporal line, and two fragments from the left side of the frontal squama are missing. A lateral segment of the coronal suture, ~18 mm long, is poorly preserved on the left side to the approximate position of the pterion. (**B**) Left temporal bone, lateral view (left) and inferior view (right). The petrous portion is missing, broken at its base from the temporal. Two small fragments of the lateral portion of the tympanic adhere to the bone as part of the medioposterior wall of the mandibular fossa and the posterior wall of the external acoustic meatus. A slender fragment (27 × 7 mm) of the greater wing of the sphenoid bone is articulated to the lower half of the temporal's anterior suture.

[1]Human Origins Program, National Museum of Natural History, Smithsonian Institution, Washington, DC 20560–0112, USA. [2]Division of Paleontology, National Museums of Kenya, P.O. Box 40658, Nairobi, Kenya. [3]Department of Paleobiology, National Museum of Natural History, Smithsonian Institution, Washington, DC 20560, USA. [4]Berkeley Geochronology Center, 2455 Ridge Road, Berkeley, CA 94709, USA. [5]Research Laboratory for Archaeology, University of Oxford, 6 Keble Road, Oxford, OX1 3QJ, UK.

*To whom correspondence should be addressed. E-mail: potts.rick@nmnh.si.edu

Downloaded from www.sciencemag.org on January 2, 2007

KNM-OL 45500 had a cranial capacity less than 800 cc. Thus, although brain size varied substantially in early- and mid-Pleistocene hominins (*1*), there was little change apparent over time in the small end of the size range.

Although small, the Olorgesailie cranium possesses characters observed in larger individuals of *H. erectus*, such as midline keeling of the frontal bone, shelf-like morphology of the posttoral sulcus, lack of torsion in the toral anterior surface, and a short temporal squama with flat superior border. KNM-OL 45500 also shows a double-arched supraorbital torus, which is more strongly developed in some mid-Pleistocene hominins, such as Bodo and Kabwe, than in Asian *H. erectus*, but is also expressed to a varying degree in Daka, Ceprano, and KNM-ER 3733 (table S1). KNM-OL 45500 lacks the deep mandibular fossa typical of Asian *H. erectus* and displays an overall morphology that would extend the known range of this species. Comparison of KNM-OL 45500 with other crania (table S1) illustrates that metric and qualitative similarities cut across temporal and spatial groups of fossil specimens. The expression of diverse combinations of traits in mid-Pleistocene hominins is also evident in previous efforts to define new taxa on the basis of single crania or small fossil samples (*10*, *11*, *26*).

The fossil's stratigraphic position is the same as excavations 1.5 km eastward that have yielded several of the densest in situ accumulations of Acheulean handaxes known in Africa (*17*). Two handaxes and several flakes consistent with Acheulean technology were recovered on the surface at the KNM-OL 45500 site, immediately downslope from it and within 20 m along the steep erosional slope at the same stratigraphic level.

Fauna associated with the Member 5/7 boundary at the handaxe sites include the abundant grazing species *Theropithecus oswaldi* and *Equus* spp. Fossils found by sieving of the sandy silt adhering to the frontal bone include amphibian bones and a single tooth of the rodent *Otomys* sp., which inhabits thick grasses in and around modern East African swamps, lakes, and rivers. Dental fragments of a suid and an elephantid, probably *Elephas recki*, were surface finds at the hominin site at the same stratigraphic level as KNM-OL 45500. Stable isotope values on paleosol carbonates indicate the prevalence of C_4 open vegetation along the ridge where the hominin was found (Fig. 2, table S2, and supporting online text).

The scarcity of fossil hominins from the African mid-Pleistocene has been problematic, given the abundance of older specimens and the rich concentrations of stone artifacts and fossil animals in mid-Pleistocene localities such as Olorgesailie. Because of their absence in diverse sediments of the Olorgesailie basin, we hypothesized that these Acheulean hominins occupied upland areas and that their fossils might be preserved in deposits along volcanic ridges connecting the upland and lowland zones (*18*). The context of KNM-OL 45500 on the edge of a lava ridge supports this hypothesis and further suggests that Acheulean toolmakers entered the lowland to obtain food and water and left numerous stone tools there, but died primarily in nonburial upland contexts.

The stratigraphic position of this small-sized individual at the same level as large Acheulean cutting tools, which required powerful detachment of massive flakes from outcrops, suggests that both large and small adults occurred in the local hominin population. KNM-OL 45500 further suggests that supraorbital morphology and crest development in the mastoid region were size-dependent and that marked size differences could occur in immediately adjacent structures. The resulting potential for highly varying combinations of traits may explain why it remains controversial to define species-specific characters and to apportion variation to distinct hominin lineages after the origin of early African *H. erectus*.

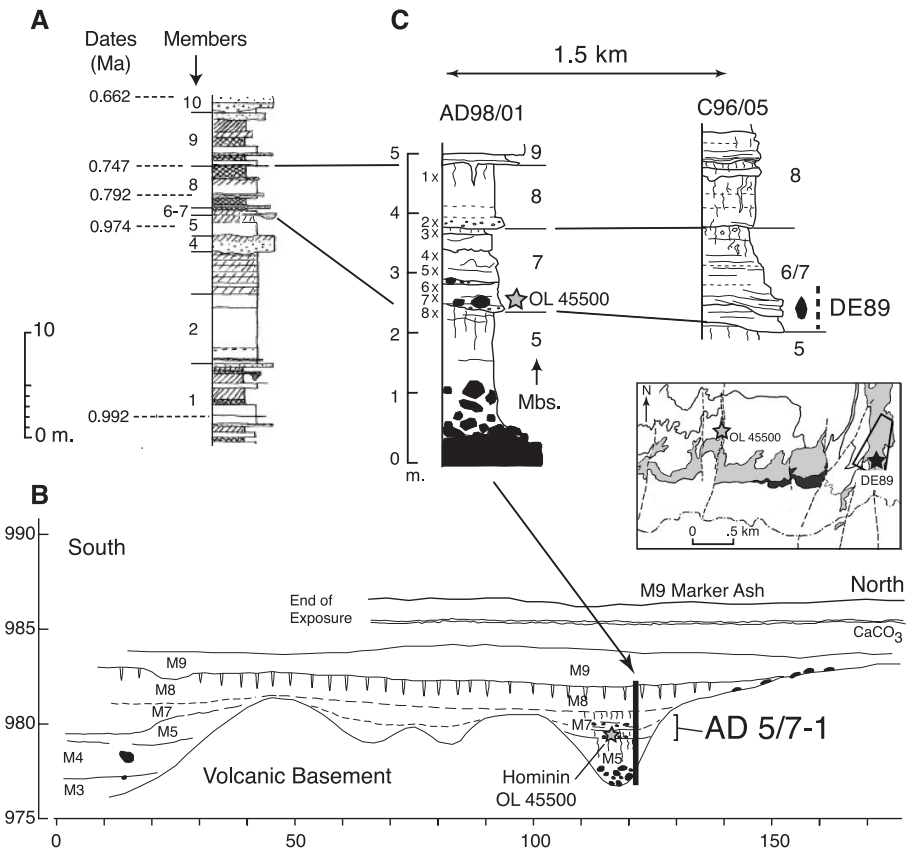


Fig. 2. Geological context of KNM-OL 45500. (**A**) Composite stratigraphic column for the lower portion of the Olorgesailie Formation, showing radiometric ages for tephra horizons in Members 1, 5, basal 9, and 10, and the Brunhes/Matuyama boundary in lower Member 8. (**B**) Panel diagram showing the context of the hominin specimen near the boundary between Members (M) 7 and 5 on the edge of a volcanic ridge (a northern extension of Lava Hump). This ridge lies immediately west of the panel and exhibits small topographic irregularities on its eastern side. Olorgesailie Formation diatomites and volcaniclastic sediments lapped onto this ridge, filling in the low areas and eventually burying the ridge. Black clasts represent volcanic boulders and cobbles derived from a higher elevation of the local basement rock and incorporated into the lower parts of Members 5 and 7 in section AD98/01. (**C**) Expanded stratigraphic section of AD98/01, showing the context of KNM-OL 45500, which occurred at the same level as the artifact concentrations 1.5 km to the east. At the handaxe site DE89 (section C96/05), the artifacts occur in channel sands that locally cut into the paleosol at the top of Member (Mb.) 5; these sands originally were defined as Member 6 but do not occur as a mappable unit outside of the Site Museum area (quadrilateral outline). To the west, the fossil KNM-OL 45500 occurred on top of the Member 5 paleosol within the Member 7 sandy silts containing reworked diatomite and volcanic cobbles. The contact between Members 6/7 and 5 is conformable except where shallow channels occur in the vicinity of the handaxe sites. Thus, the age of this contact and the hominin fossil is estimated to lie between ~970 and 900 ka. The stratigraphic positions of samples used for isotopic analysis (table S2 and supporting online text) are indicated by 1x to 8x.

References and Notes

1. S. C. Antón, *Yearb. Phys. Anthropol.* **46**, 126 (2003).
2. E. Tamrat, N. Thouveny, M. Taïeb, N. D. Opdyke, *Palaeogeogr. Palaeoclimatol. Palaeoecol.* **114**, 273 (1995).
3. T. D. White, in *Encyclopedia of Human Evolution and Prehistory*, E. Delson, I. Tattersall, J. A. Van Couvering, A. S. Brooks, Eds. (Garland, New York, 2000), pp. 486–489.

Downloaded from www.sciencemag.org on January 2, 2007

4. B. Asfaw *et al.*, *Nature* **416**, 317 (2002).
5. E. Abbate *et al.*, *Nature* **393**, 458 (1998).
6. G. C. Conroy, C. J. Jolly, D. Cramer, J. E. Kalb, *Nature* **276**, 67 (1978).
7. G. P. Rightmire, *Am. J. Phys. Anthropol.* **61**, 245 (1983).
8. G. P. Rightmire, *J. Hum. Evol.* **31**, 21 (1996).
9. J. J. Hublin, in *Human Roots: Africa and Asia in the Middle Pleistocene*, L. Barham, K. Robson-Brown, Eds. (Western Academic & Specialist Press, Bristol, UK, 2001), pp. 99–121.
10. J.-L. Arsuaga *et al.*, *J. Hum. Evol.* **37**, 431 (1999).
11. G. Manzi, F. Mallegni, A. Ascenzi, *Proc. Natl. Acad. Sci. U.S.A.* **98**, 10011 (2001).
12. G. Manzi, E. Bruner, P. Passarello, *J. Hum. Evol.* **44**, 731 (2003).
13. W. H. Gilbert, T. D. White, B. Asfaw, *J. Hum. Evol.* **45**, 255 (2003).
14. G. P. Rightmire, *Evol. Anthropol.* **6**, 218 (1998).
15. I. Tattersall, *J. Hum. Evol.* **15**, 165 (1986).
16. M. H. Wolpoff, A. G. Thorne, J. Jelínek, Y. Zhang, *Cour. Forschungsinst. Senckenb.* **171**, 341 (1994).
17. G. Ll. Isaac, *Olorgesailie: Archaeological Studies of a Middle Pleistocene Lake Basin in Kenya* (Univ. of Chicago Press, Chicago, IL, 1977).
18. R. Potts, A. K. Behrensmeyer, P. Ditchfield, *J. Hum. Evol.* **37**, 747 (1999).
19. A. Deino, R. Potts, *J. Geophys. Res.* **95,** 8453 (1990).
20. L. Tauxe, A. L. Deino, A. K. Behrensmeyer, R. Potts, *Earth Planet. Sci. Lett.* **109**, 561 (1992).
21. Y. Hou *et al.*, *Science* **287**, 1622 (2000).
22. A. M. Sarna-Wojcicki, M. S. Pringle, J. Wijbrans, *J. Geophys. Res.* **105**, 21431 (2000).
23. S. C. Antón, *Am. J. Phys. Anthropol.* **102**, 497 (1997).
24. L. Gabunia *et al.*, *Science* **288**, 1019 (2000).
25. S. C. Antón, *J. Hum. Evol.* **46**, 335 (2004).
26. F. Mallegni *et al.*, *C. R. Paleovol.* **2**, 153 (2003).

27. Olorgesailie research is conducted in collaboration with the National Museums of Kenya (NMK), with excavation licenses granted by the Kenyan government. This work was funded by NSF (grant BCS-0218511) and the Smithsonian Institution's Human Origins Program. We thank I. O. Farah, M. G. Leakey, E. Mbua, M. Muungu, S. N. Muteti, and the staff of the NMK Palaeontology Division for support. The analysis and manuscript benefited from discussions with S. Antón, F. Spoor, and B. Wood.

Supporting Online Material

www.sciencemag.org/cgi/content/full/305/5680/75/DC1
SOM Text
Tables S1 and S2
References

8 March 2004; accepted 25 May 2004

Evidence for Precipitation on Mars from Dendritic Valleys in the Valles Marineris Area

Nicolas Mangold,[1*] Cathy Quantin,[2] Véronique Ansan,[1] Christophe Delacourt,[2] Pascal Allemand[2]

Dendritic valleys on the plateau and canyons of the Valles Marineris region were identified from Thermal Emission Imaging System (THEMIS) images taken by Mars Odyssey. The geomorphic characteristics of these valleys, especially their high degree of branching, favor formation by atmospheric precipitation. The presence of inner channels and the maturity of the branched networks indicate sustained fluid flows over geologically long periods of time. These fluvial landforms occur within the Late Hesperian units (about 2.9 to 3.4 billion years old), when Mars was thought to have been cold. Our results suggest a period of warmer conditions conducive to hydrological activity.

The formation of valley networks on Mars has been the subject of considerable scientific debate (*1–4*). Valleys were attributed to fluvial erosion implying a warm and wet climate on early Mars (*5*), possibly conducive to biological activity (*6*). Several recent observations argue in favor of such conditions on early Mars (*7*, *8*), but valley networks could also have formed by water-lubricated debris flows (*4*), hydrothermal activity (*9*, *10*), or groundwater sapping (*11–13*) due to geothermal activity (*14*), and these hypotheses do not require conditions warmer than the current cold climate.

Here, we describe terrestrial-like dendritic valleys identified using THEMIS images (*15*) of the Mars Odyssey mission. These valleys are located in the Valles Marineris region (Fig. 1) on the plateau west of Echus Chasma (Fig. 2) and on the inner plateau west of Melas Chasma (Fig. 3). These landforms occur within Late Hesperian units (*16*), about 2.9 to 3.4 billion years old (*17*); they are thus unexpectedly younger than the Noachian (*16*) period, which is considered to be the potential primitive warm period (*4*).

The plateau west of Echus Chasma (0°N, 81°W) is covered by densely branched valleys that are frequently sinuous and extend over tens of kilometers (Fig. 2). Infrared (IR) images taken at night by THEMIS (Fig. 2A) show mainly intrinsic thermal properties of the ground (*15*). Valleys buried under loose material are outlined by variations of the thermal signal and resemble terrestrial deserts where sand covers the floor of dry valleys (fig. S1). On drainage basin G, the main valley is larger upstream than downstream close to the mouth, implying a thicker mantling at this location. With the exception of this place, most valleys have widths increasing from their sources to their mouth, as seen in terrestrial valleys. An IR image taken during the day by THEMIS shows that these dendritic valleys have their heads scattered at random points on the plateau (Fig. 2C). Hills

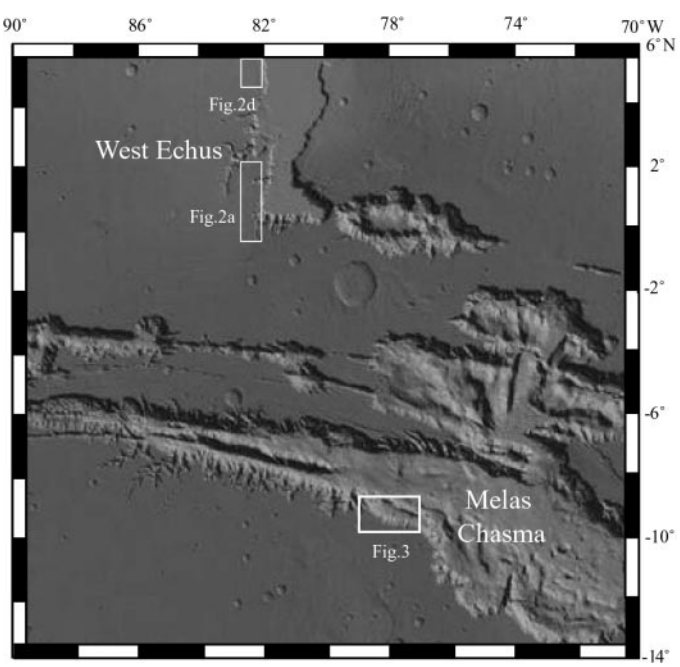


Fig. 1. MOLA shaded relief map of West Valles Marineris and the neighboring canyons. White squares indicate valley networks observed over Hesperian geologic units on THEMIS images of Figs. 2 and 3.

[1]Laboratoire IDES, UMR CNRS and Université Paris-Sud, Orsay Campus, 91405 Orsay, France. [2]Laboratoire des Sciences de la Terre, UMR CNRS UCB Lyon 1 and ENS Lyon, La Doua Campus, 69622 Villeurbanne, France.

*To whom correspondence should be addressed. E-mail: mangold@geol.u-psud.fr

Downloaded from www.sciencemag.org on January 2, 2007